UCSF
UC San Francisco Previously Published Works

Title

Erk Negative Feedback Control Enables Pre-B Cell Transformation and Represents a Therapeutic Target in Acute Lymphoblastic Leukemia

Permalink

https://escholarship.org/uc/item/4dd9q5xn

Journal

Cancer Cell, 28(1)

ISSN

1535-6108

Authors

Shojaee, S
Caeser, R
Buchner, M
et al.

Publication Date

2015-07-13

DOI

10.1016/j.ccell.2015.05.008

Peer reviewed

eScholarship.org Powered by the California Digital Library
University of California

Article

Cancer Cell

Erk Negative Feedback Control Enables Pre-B Cell Transformation and Represents a Therapeutic Target in Acute Lymphoblastic Leukemia

Highlights

- Robust negative regulation of Erk enables transformation of pre-B cells
- High Erk feedback activity predicts poor clinical outcome of patients with ALL
- Deletion of Erk feedback genes protects against pre-B cell transformation
- Small molecule inhibition of the Erk-phosphatase DUSP6 kills patient ALL cells

Authors

Seyedmehdi Shojaee, Rebecca Caeser, Maike Buchner, ..., Ari Melnick, Steven M. Kornblau, Markus Müschen

Correspondence

markus.muschen@ucsf.edu

In Brief

Shojaee et al. show that successful transformation of pre-B cells to pre-B acute lymphoblastic leukemia (ALL) requires negative feedback regulation of Erk signaling and inhibiting this feedback selectively kills pre-B ALL cells, suggesting negative feedback regulation of oncogenes as a vulnerability in human ALL.

Accession Numbers

GSE34832
GSE34834
GSE34833
GSE23743
GSE21664

Shojaee et al., 2015, Cancer Cell *28*, 1–15
July 13, 2015 ©2015 Elsevier Inc.
http://dx.doi.org/10.1016/j.ccell.2015.05.008

CellPress

Please cite this article in press as: Shojaee et al., Erk Negative Feedback Control Enables Pre-B Cell Transformation and Represents a Therapeutic Target in Acute Lymphoblastic Leukemia, Cancer Cell (2015), http://dx.doi.org/10.1016/j.ccell.2015.05.008

Cancer Cell
Article

CellPress

Erk Negative Feedback Control Enables Pre-B Cell Transformation and Represents a Therapeutic Target in Acute Lymphoblastic Leukemia

Seyedmehdi Shojaee,[1] Rebecca Caeser,[1,12] Maike Buchner,[1] Eugene Park,[12] Srividya Swaminathan,[1] Christian Hurtz,[1] Huimin Geng,[1] Lai N. Chan,[1] Lars Klemm,[1] Wolf-Karsten Hofmann,[2] Yi Hua Qiu,[3] Nianxiang Zhang,[4] Kevin R. Coombes,[4] Elisabeth Paietta,[5] Jeffery Molkentin,[6] H. Phillip Koeffler,[7,8] Cheryl L. Willman,[9] Stephen P. Hunger,[10] Ari Melnick,[11] Steven M. Kornblau,[3] and Markus Müschen[1,*]

[1]Department of Laboratory Medicine, University of California San Francisco, San Francisco, CA 94143, USA
[2]III. Medizinische Klinik, Medizinische Fakultät Mannheim, Universität Heidelberg, Heidelberg 68167, Germany
[3]Department of Leukemia, The University of Texas M.D. Anderson Cancer Center, Houston, TX 77030, USA
[4]Department of Bioinformatics and Computational Biology, The University of Texas M.D. Anderson Cancer Center, Houston, TX 77030, USA
[5]Albert Einstein College of Medicine, Bronx, NY 10466, USA
[6]Howard Hughes Medical Institute and Cincinnati Children's Hospital, University of Cincinnati, Cincinnati, OH 45247, USA
[7]Division of Hematology and Oncology, Cedars Sinai Medical Center, Los Angeles, CA 90095, USA
[8]Cancer Science Institute of Singapore, National University of Singapore, Singapore 117599, Singapore
[9]Department of Pathology, University of New Mexico Cancer Center, Albuquerque, NM 87102, USA
[10]Division of Oncology, Children's Hospital of Philadelphia, Philadelphia, PA 19104, USA
[11]Departments of Medicine and Pharmacology, Weill Cornell Medical College, New York, NY 10065, USA
[12]Department of Haematology, University of Cambridge, Cambridge CB2 0AH, UK
*Correspondence: markus.muschen@ucsf.edu
http://dx.doi.org/10.1016/j.ccell.2015.05.008

SUMMARY

Studying mechanisms of malignant transformation of human pre-B cells, we found that acute activation of oncogenes induced immediate cell death in the vast majority of cells. Few surviving pre-B cell clones had acquired permissiveness to oncogenic signaling by strong activation of negative feedback regulation of Erk signaling. Studying negative feedback regulation of Erk in genetic experiments at three different levels, we found that *Spry2*, *Dusp6*, and *Etv5* were essential for oncogenic transformation in mouse models for pre-B acute lymphoblastic leukemia (ALL). Interestingly, a small molecule inhibitor of DUSP6 selectively induced cell death in patient-derived pre-B ALL cells and overcame conventional mechanisms of drug-resistance.

INTRODUCTION

Pre-B acute lymphoblastic leukemia (ALL) represents the most frequent type of cancer in children and is frequent in adults as well. Despite greatly improved outcomes for patients over the past four decades (Bhojwani and Pui, 2013), pre-B ALL remains one of the leading causes of person-years of life lost in the United States (362,000 years in 2010; National Center of Health Statistics; Murphy et al., 2013), which is attributed to the high incidence of ALL in children. Activating lesions in the RAS pathway (~50%; Zhang et al., 2011) and oncogenic tyrosine kinases (e.g., BCR-ABL1; ~25%) result in hyperactivation of Erk and other MAP kinases (MAPK). The BCR-ABL1 tyrosine kinase in Philadelphia chromosome (Ph^+) ALL represents the most frequent oncogene (~30% of ALL cases in adults) and also defines the subgroup of patients with the worst clinical outcome (Fielding, 2010). In addition to classical Ph^+ ALL harboring the BCR-ABL1 rearrangement, recent studies discovered a Ph-like

Significance

Targeted therapy of cancer typically focuses on the development of agents that will suppress the signaling strength of transforming oncogenes below a minimum threshold that is required to sustain survival and proliferation. In this study, we tested the concept that besides the oncogene itself, factors that enable permissiveness of normal pre-B cells to oncogenic signaling represent a class of therapeutic targets for the treatment of acute lymphoblastic leukemia (ALL). Studying negative feedback control of Erk at three levels (SPRY2, DUSP6, and ETV5), we showed that intact Erk feedback regulation is critical for permissiveness of pre-B cells to oncogenic transformation. Albeit counterintuitive, our findings identify negative feedback regulation of oncogenes as a vulnerability in human ALL.

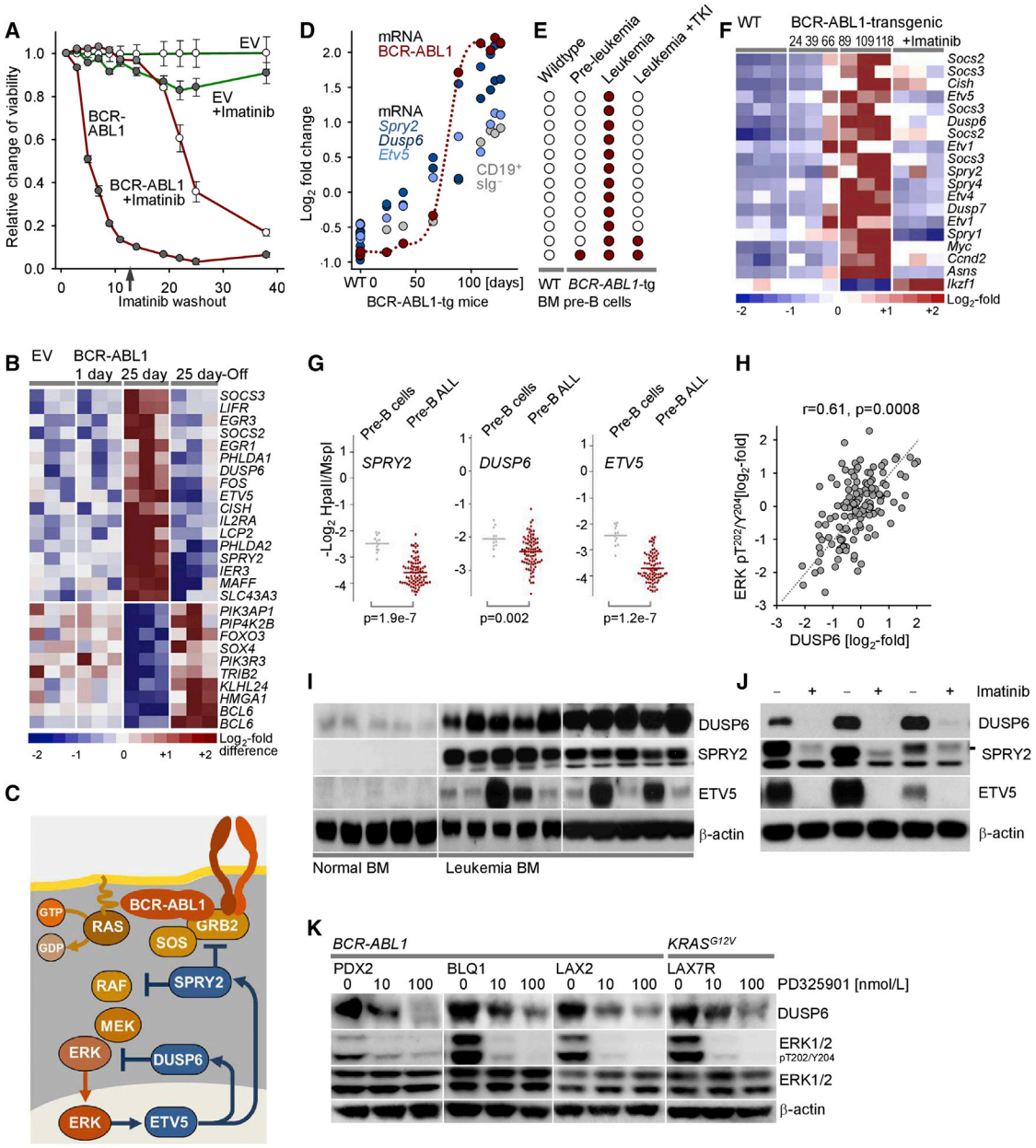

Figure 1. Activation of Negative Control Correlates with Pre-B Cell Transformation

(A) Human bone marrow pre-B cell cultures were transduced with retroviral BCR-ABL1^{GFP} and GFP EV. The fractions of GFP-expressing cells were measured by flow cytometry and fold-change of GFP$^+$ cells and are depicted (y axis). The x axis represents days after transduction. The error bars represent SD.

(B) Gene expression changes upon acute BCR-ABL1 activation (TKI-washout; 1 day), full transformation of pre-B cells (25 day), and acute BCR-ABL1 kinase inhibition (TKI readdition; 25 day-Off) were monitored by microarray analysis.

(C) Schematic of negative feedback control of Erk signaling molecules studied here.

(D) Progressive leukemic transformation of pre-B cells in BCR-ABL1-transgenic mice was monitored by measurement of BCR-ABL1 mRNA levels and peripheral blood B cell precursors (CD19$^+$ surface Ig$^-$) relative to the mRNA levels of *Spry2*, *Dusp6*, and *Etv5*.

(E) Single pre-B cells from the bone marrow of wild-type controls, young BCR-ABL1-transgenic mice (no detectable disease), BCR-ABL1-transgenic mice with overt leukemia before and after in vivo treatment with Nilotinib (TKI) were sorted into PCR tubes and the BCR-ABL1 transcripts were amplified by RT-PCR. The positive cells were depicted as red circles.

(F) Gene expression changes during progressive malignant transformation of pre-B cells in BCR-ABL1-transgenic mice are depicted as a heatmap.

(G) Results of CpG methylation analyses are shown for promoters of *SPRY2*, *DUSP6*, and *ETV5* in CD19$^+$ bone marrow pre-B cells from healthy donors (n = 12) and bone marrow biopsies from patients with Ph$^+$ ALL (n = 83). The p values were calculated from two-sided Mann-Whitney Wilcoxon test.

(H) RPPA data from pre-B ALL samples in the adult MDACC 1983–2007 clinical trial for ERK phosphorylation (T^{202}/Y^{204}) and DUSP6 protein expression were plotted (n = 126). The correlation coefficient was calculated using the Pearson correlation coefficient.

(legend continued on next page)

subset of ALL that is frequent in children and young adults (Roberts et al., 2014) and shares central biological and clinical characteristics with Ph^+ ALL. Ph-like ALL is driven by a diverse spectrum of oncogenic tyrosine kinases and cytokine receptors (Roberts et al., 2012). Therapy with tyrosine kinase inhibitors (TKI) in Ph^+ or Ph-like ALL typically achieves complete remission of leukemia. However, these ALL subtypes frequently relapse under TKI-treatment (Druker et al., 2001).

Lesions that drive oncogenic Erk activation include activating mutations of *NRAS*, *KRAS*, *BRAF*, and *PTPN11* as well as inactivating mutations of *NF1* (Zhang et al., 2011). Lesions in the Erk pathway are frequently found in relapse ALL samples and are drivers of ALL relapse (Irving et al., 2014). Activated Erk translocates to the nucleus and drives transcriptional activation of proliferation via *FOS*, *JUN*, and *MYC* as well as its own negative feedback at three levels: (1) The sprouty family signaling inhibitor SPRY2 negatively regulates activation of *RAS* (Hanafusa et al., 2002). (2) The dual specificity phosphatase 6 (DUSP6) dephosphorylates Erk (Tanoue et al., 2000). And (3) through translocation to the nucleus, Erk cooperates with PEA3 Ets transcription factors including ETV1, ETV4, and ETV5 that function as transcriptional activators of *DUSP6* and *SPRY2* (Chi et al., 2010; Znosko et al., 2010; Hollenhorst et al., 2011).

Targeted therapy of cancer typically focuses on the development of agents that withdraw a transforming oncogene that cancer cells have become addicted to. In this study, we tested the concept that besides the oncogene itself, additional factors confer permissiveness to oncogenic signaling and enable a normal cell to engage with and tolerate an oncogenic level of signaling strength. These factors would represent vulnerabilities that can be leveraged in anti-cancer therapies and, hence, be considered as a class of therapeutic targets.

RESULTS

Our hypothesis was based on our finding that acute activation of oncogenes (e.g., BCR-ABL1 and $NRAS^{G12D}$) induced cell death in the vast majority of human pre-B cells (Figures 1A, S1A, and S1B). Only a small fraction survived acute activation of oncogene signaling and eventually gave rise to malignant transformation after a delay of more than 3 weeks. A phenotypic comparison at the gene expression level between human pre-B cells with acute activation of BCR-ABL1 (1 day) and complete transformation by BCR-ABL1 (25 days) revealed that transformed pre-B ALL clones evolved high expression levels of negative regulators of Erk, including *DUSP6*, *ETV5*, and *SPRY2* (Figures 1B and 1C). While activation of BCR-ABL1 in the parental pre-B cell culture caused cell death, the transformed pre-B cell clones were addicted to BCR-ABL1 after 25 days and had acquired sensitivity to TKI. Interestingly, TKI-treatment for 1 hr (25 days-Off) was sufficient to erase high expression levels of negative control molecules (Figure 1B).

Pre-B Cells in BCR-ABL1-Transgenic Mice Are Not Readily Permissive to Oncogenic Transformation

In BCR-ABL1-transgenic mice, all pre-B cells carry the BCR-ABL1 transgene. However, leukemia invariably develops only from a very small number of pre-B cell clones as a monoclonal disease in most cases (Voncken et al., 1992). The BCR-ABL1-transgenic mouse model suggests that the vast majority of pre-B cells are not readily permissive to oncogenic transformation. BCR-ABL1-transgenic mice gave rise to overt pre-B ALL (accumulation of peripheral blood $CD19^+$ surface Ig^- blasts) only after about 90 days and BCR-ABL1 mRNA levels remained undetectable in the bone marrow until about 60 days of age (Figure 1D). Single-cell RT-PCR analysis revealed that the BCR-ABL1-transgene was transcriptionally silent in 11 of 12 pre-B cells sorted from pooled bone marrows of disease-free "pre-leukemic" BCR-ABL1-transgenic mice at a young age (n = 3). In BCR-ABL1-transgenic mice with full-blown leukemia, virtually all bone marrow pre-B cells expressed the BCR-ABL1-transgene and became addicted to the oncogene: subsequent TKI treatment selectively killed these cells and spared pre-B cells carrying a transcriptionally silent BCR-ABL1-transgene (Figure 1E). Comparing pre-leukemic and fully transformed pre-B cells from BCR-ABL1-transgenic mice, we found that leukemic transformation was paralleled by strong activation of genes encoding negative control of Erk (*Dusp6*, *Spry2*, and *Etv5*; Figure 1F). Expression of these molecules was sensitive to TKI-treatment in vivo. Based on these findings, we hypothesize that activation of BCR-ABL1 and other oncogenes in pre-B cells imposes selective pressures in favor of clones that have evolved robust negative control of Erk. In the absence of robust negative control, pre-B cells are not permissive to oncogene activation and are counterselected from the pre-leukemic repertoire in BCR-ABL1-transgenic mice (Figure 1E).

Erk Negative Control Is Selectively Activated in Human Pre-B ALL Cells

Recent studies found that negative feedback regulators of Erk (DUSP6, ETV5, and SPRY2) are frequently inactivated in solid tumors (Xu et al., 2005; Shaw et al., 2007; Schutzman and Martin, 2012; Wong et al., 2012) and mature B cell lymphoma (Frank et al., 2009) and have an important role as tumor suppressors in attenuating oncogenic signaling (Courtois-Cox et al., 2006). Surprisingly, however, primary samples from patients with pre-B ALL (n = 83) showed significantly lower levels of CpG methylation in the promoters of *DUSP6*, *ETV5*, and *SPRY2* compared to normal pre-B cells (Figure 1G). These results suggest that pre-B ALL cells, unlike normal pre-B cells, are poised to express negative regulators of Erk. To measure activity of Erk negative regulation in a larger cohort of patient-derived samples, reverse phase protein array (RPPA) data from a clinical trial for adults with pre-B ALL were studied for protein levels of DUSP6 and phospho-ERK-T^{202}/Y^{204}. RPPA measurements revealed a strong positive correlation between expression levels

(I) Western blot analysis for expression of DUSP6, SPRY2, and ETV5 in normal $CD19^+$ bone marrow pre-B cells (n = 5) and patient-derived pre-B ALL (n = 10) are shown with β-actin as loading control.
(J) Western blot analysis for expression of DUSP6, SPRY2, and ETV5 in Ph^+ pre-B ALL cases (±Imatinib 10 μmol/l) is shown using β-actin as loading control.
(K) Patient derived ALL cells were treated with or without the MEK inhibitor PD0325901 for 2 hr. Western blot for DUSP6 and total and phospho-ERK were performed using β-actin as loading control. See also Figure S1.

of phospho-ERK-T^{202}/Y^{204} and its negative regulator DUSP6 (Figure 1H). RPPA protein levels for DUSP6 also correlated with activity of other MAPK including p38α (MAPK14) and MEK (MAP2K1; Figure S1C). Western blot analyses confirmed that patient-derived pre-B ALL cells express DUSP6, SPRY2, and ETV5 at much higher levels than bone marrow pre-B cells (Figure 1I). Consistent with dynamic changes of mRNA levels during BCR-ABL1-mediated transformation of human (Figure 1B) and mouse pre-B cells (Figure 1F), high protein levels of negative regulators were sensitive to Imatinib treatment in human Ph^+ ALL cells (Figure 1J). Likewise, MEK kinase inhibition not only abolished Erk activity, but also reduced DUSP6 protein levels by 4- to 25-fold (Figure 1K).

Robustness of Erk Negative Control Is a Predictor of Poor Clinical Outcome in B Cell-Lineage, but Not Myeloid Leukemia

Previous work demonstrated that negative feedback inhibition of Erk signaling induces oncogene-induced senescence and represents a barrier against malignant transformation (Courtois-Cox et al., 2006), which is disabled in many types of cancer (Pratilas et al., 2009; Frank et al., 2009). In human pre-B ALL, however, negative control of Erk is constitutively active (Figure 1I). We therefore tested whether activity of this pathway correlates with the course of disease and clinical outcome of patients with pre-B ALL. To this end, we studied *DUSP6* mRNA levels as a potential predictor of outcome for adults with Ph^+ ALL, using acute myeloid leukemia (AML) patients as a reference. For these analyses, patients were separated into two groups based on higher or lower than median mRNA levels of *DUSP6* at the time of diagnosis. In AML, higher than median levels of *DUSP6* associated with a trend toward longer overall survival (Figure 2A), however, in contrast, higher than median *DUSP6* levels strongly correlated with shorter overall survival for adults with pre-B ALL (Figure 2A). Multivariate analyses using achievement of complete remission (CR) as an established risk factor, showed that high *DUSP6* mRNA levels represent independent predictors of clinical outcome in adults with pre-B ALL (Figure 2A). We then combined each three activators (MAPK; *MAPK1*, *NRAS*, and *MAP2K1*) and negative regulators (DUSP; *DUSP6*, *SPRY2*, and *ETV5*) into a six-gene outcome predictor (Figure 2B). The potential usefulness of the DUSP-MAPK outcome predictor is exemplified based on two cohorts: Among adults with Ph^+ ALL, none of the patients with $DUSP^{High}/MAPK^{Low}$ profile survived 15 months after diagnosis, whereas ~50% of patients with $DUSP^{Low}/MAPK^{High}$ were still alive 8 years after diagnosis (Figure 2B). Similarly, in the pediatric high-risk ALL trial, patients with a $DUSP^{Low}/MAPK^{High}$ profile represented a group with a particularly favorable outcome (Figure 2B). Multivariate analyses confirmed that the DUSP/MAPK profile represents an independent predictor of clinical outcome (Figure S2). In contrast to B cell-lineage ALL, the combined analysis of DUSP-MAPK profiles had the opposite outcome in AML patients (Figure 2B). These findings suggest that high expression levels of Erk negative regulators represent a powerful, albeit B cell lineage-specific, biomarker with potential uses in risk stratification of pre-B ALL patients.

To test potential divergent lineage-specific functions of DUSP6, we isolated bone marrow from $Dusp6^{-/-}$ mice (Maillet et al., 2008) and wild-type controls and transformed B cell lineage and myeloid progenitor cells with BCR-ABL1 (Figure 2C). Interestingly, levels of both Erk activity and DUSP6 expression differed between B cell and myeloid lineage leukemia cells, suggesting distinct lineage-specific Erk activity regulation (Figure 2D). For colony forming assays, $Dusp6^{+/+}$ and $Dusp6^{-/-}$ B cell lineage and myeloid lineage leukemia cells were plated in methylcellulose. Consistent with a role of DUSP6 as a tumor suppressor in multiple types of cancer (Courtois-Cox et al., 2006; Pratilas et al., 2009; Frank et al., 2009), colony formation of $Dusp6^{-/-}$ myeloid leukemia was increased compared to wild-type controls (Figure 2E). In contrast, colony formation of $Dusp6^{-/-}$ B cell lineage leukemia was reduced (Figure 2E), supporting the concept that, unlike other types of cancer, DUSP6 enables malignant transformation in B cell lineage ALL.

DUSP6-Mediated Negative Control of Erk Signaling Is Essential for $NRAS^{G12D}$-Mediated Pre-B Cell Transformation

To determine the significance of Erk negative regulation in RAS-driven ALL in a genetic experiment, we transduced $Dusp6^{+/+}$ and $Dusp6^{-/-}$ IL7-dependent pre-B cells with a doxycycline-inducible vector system for regulatable expression of oncogenic $NRAS^{G12D}$. While expression of $NRAS^{G12D}$ was able to transform $Dusp6^{+/+}$ pre-B cells and increase colony formation, $NRAS^{G12D}$ failed to transform or induce colony formation of $Dusp6^{-/-}$ pre-B cells (Figure 3A). Induction of $NRAS^{G12D}$ caused a moderate increase in Erk phosphorylation in the presence of *Dusp6*. In $Dusp6^{-/-}$ pre-B cells, Erk is constitutively active and massively increased upon induction of $NRAS^{G12D}$ (Figure 3B). Reconstitution of $Dusp6^{-/-}$ $NRAS^{G12D}$ pre-B cells with the wild-type DUSP6, but not catalytically inactive $DUSP6^{C293S}$, corrected massive hyperactivation of Erk (Figures 3C and 3D). Collectively, these findings establish that DUSP6 is required to calibrate Erk signaling downstream of oncogenic $NRAS^{G12D}$ and that DUSP6 is essential for RAS-driven B cell lineage ALL. Interestingly, acute activation of $NRAS^{G12D}$ in $Dusp6^{+/+}$ pre-B cells caused a minor increase of cellular senescence and had no significant impact on cell viability. In the absence of *Dusp6*, however, activation of $NRAS^{G12D}$ caused massive senescence and acute toxicity (Figures 3E and 3F), highlighting the critical importance of DUSP6-dependent negative regulation in buffering Erk signal strength in transformed murine pre-B cells. These findings are also relevant to human pre-B ALL. Transduction of $KRAS^{G12V}$- and *MLL-AF4*-driven human ALL cells with small hairpin RNA vectors against DUSP6 resulted in ~50% reduction of DUSP6. While the resulting increase in Erk activity was minor, it was sufficient to significantly reduce colony forming capacity of the two pre-B ALL cases (Figures 3G and 3H). These findings suggest that human ALL cells are uniquely sensitive to even small imbalances in Erk signaling.

Transduction of $Dusp6^{+/+}$ pre-B cells with $NRAS^{G12D}$ induced leukemic transformation and fatal disease in transplant recipients (Figure 3I). $Dusp6^{-/-}$ pre-B cells transduced with $NRAS^{G12D}$, however, failed to initiate lethal leukemia in transplant recipients (Figure 3I). In multiple tumor types, DUSP6-mediated feedback inhibition of Erk induces cellular senescence and represents a barrier against RAS-driven malignant transformation (Courtois-Cox et al., 2006). Our findings here reveal that

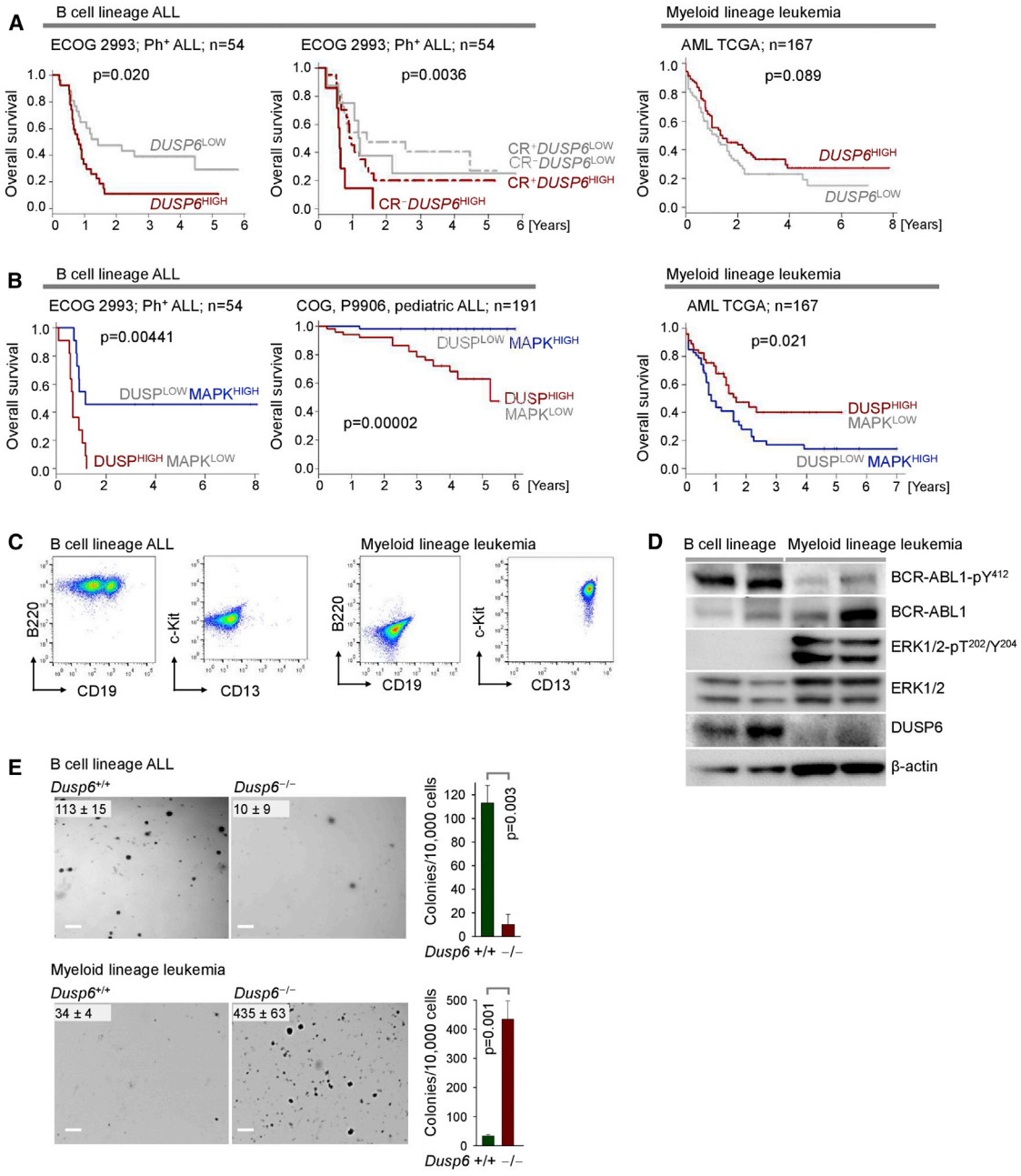

Figure 2. B Cell-Specific Role of Erk-Negative Control in Leukemia

(A) *DUSP6* mRNA levels were studied in adult patients with Ph+ ALL (ECOG 2993; n = 54) at the time of diagnosis as a potential predictor of outcome. The AML patient samples (AML TCGA; n = 167) were similarly studied as a reference. The patients were separated into two groups based on higher or lower than median mRNA levels of *DUSP6*. Also a multivariate analysis was performed using *DUSP6* mRNA levels and achievement of CR as an established risk factor. The p values were calculated from log-rank test.

(B) Expression levels of three activators (MAPK; *MAPK1*, *NRAS*, and *MAP2K1*) and three negative regulators (DUSP; *DUSP6*, *SPRY2*, and *ETV5*) of Erk signaling were combined into a six-gene outcome predictor. The DUSP-MAPK outcome predictor was used for adult patients with Ph+ ALL (ECOG E2993; n = 55) and pediatric patients with high-risk ALL (COG P9906; n = 191). The patients with AML (AML TCGA; n = 167) were similarly analyzed as a reference. The p values were calculated from log-rank test.

(C–E) B cell lineage and myeloid progenitor cells from *Dusp6*$^{-/-}$ and wild-type mice were transformed with BCR-ABL1. The transformed cells were analyzed for their expression of lineage cell surface markers by flow cytometry (C); their exppression of DUSP6, total and phosphorylated ERK1/2, and BCR-ABL1 by western blot (D); and colony formation capacity plated in methylcellulose (E). β-actin was used as loading control in the western blot. The scale bars represent 1 mm. The error bars represent SD, and p values were calculated from t test. See also Figure S2.

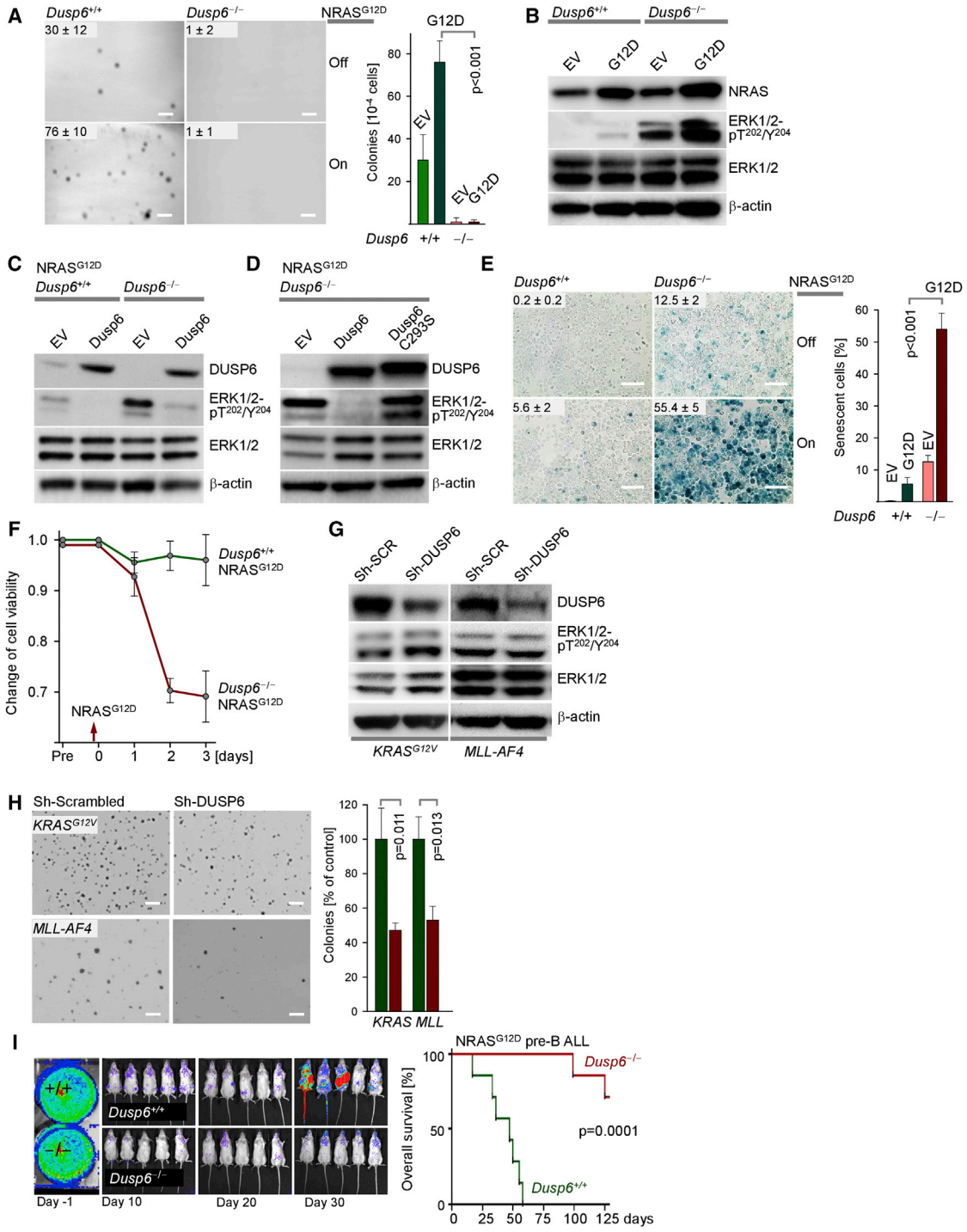

Figure 3. Dusp6 Negative Control of Erk Is Essential for NRAS^{G12D}-Mediated Pre-B Cell Transformation

(A) *Dusp6*$^{+/+}$ and *Dusp6*$^{-/-}$ IL7-dependent pre-B cells were transduced with a doxycycline-inducible vector system for regulatable expression of oncogenic NRAS^{G12D}. The cells were plated in methylcellulose to study colony formation in the presence and absence of NRAS^{G12D}. The scale bars represent 1 mm. The p value was calculated from t test.

(B) Western blot analysis on NRAS^{G12D} transduced cells for NRAS and total and phosphorylated ERK1/2 using β-actin as loading control.

(C) NRAS^{G12D} transduced *Dusp6*$^{+/+}$ and *Dusp6*$^{-/-}$ pre-B cells were transduced with either EV or wild-type DUSP6 and studied by western blot.

(D) NRAS^{G12D} transduced *Dusp6*$^{-/-}$ pre-B cells were transduced with EV, wild-type DUSP6, or catalytically inactive (DUSP6^{C293S}) and studied by western blot.

(E) *Dusp6*$^{+/+}$ and *Dusp6*$^{-/-}$ pre-B cells were induced to express NRAS^{G12D} and stained for senescence-associated β-galactosidase activity (pH 5.5) to label senescent cells. The scale bars represent 50 μm. The p value was calculated from t test.

(F) Viability of *Dusp6*$^{+/+}$ and *Dusp6*$^{-/-}$ pre-B cells was measured upon induction of NRAS^{G12D}.

(legend continued on next page)

DUSP6-mediated negative regulation of Erk represents a critical lineage-specific vulnerability in B cell lineage ALL.

Genetic Analysis of Erk Negative Control in Pre-B Cell Transformation

These findings suggest that effector molecules of Erk negative control may represent a class of therapeutic targets for the treatment of human B cell lineage ALL. For this reason, we measured functional consequences of *Dusp6*- and *Etv5*-deficiency as well as Cre-mediated deletion of *Spry2* in mouse models of pre-B ALL based on $NRAS^{G12D}$ and BCR-ABL1-mediated transformation. Bone marrow pre-B cells from $Dusp6^{-/-}$ (Maillet et al., 2008), $Etv5^{-/-}$ (Chen et al., 2005), and $Spry2^{fl/fl}$ (Shim et al., 2005) mice and wild-type controls were transformed with retroviral $NRAS^{G12D}$ or BCR-ABL1. In addition, $Spry2^{fl/fl}$ pre-B ALL cells were transduced with a 4-hydroxy tamoxifen (4-OHT) inducible form of Cre for deletion of LoxP-flanked *Spry2* alleles.

Loss of *Dusp6*, *Etv5*, or *Spry2* caused a number of prominent gene expression changes, many of which were shared among the three (Figures 4A and S3A). For instance, loss of *Dusp6*, *Etv5*, or *Spry2* commonly resulted in increased expression of the p53-related tumor suppressors *Cdkn2a* (*Arf*), *Btg2*, and *Cd82* (Figure 4A). Pre-B ALL cells lacking robust Erk negative control acquired multiple determinants of myeloid, monocytic, and mast cell lineages (e.g., *Mcpt2*, IgE Fc receptors, *Ccl2*, *Ccl3*, and *Csfr2b*) at the expense of pre-B cell specific molecules (*Ighm*, *Ms4a1*, *Igh*, *Igk*, *Il7r*, *Dntt*, *Bank1*, *Rag1*, *Rag2*, and *Vpreb1*; Figure 4A). These findings are consistent with lineage-specific effects of Erk negative control. Together with the phenotypic shift of $Dusp6^{-/-}$ pre-B ALL cells to a myeloid/mast cell gene expression pattern, these findings suggest that pre-B ALL cells are dependent on robust Erk negative control, whereas myeloid leukemia cells proliferate more vigorously in its absence (Figures 2D, S3B, and S3C). In support of the concept that pre-B ALL cells are uniquely sensitive to hyperactive Erk, a recent study identified a checkpoint at the pre-B cell stage that negatively selects normal pre-B cell clones with elevated Erk activity (Limnander et al., 2011).

Previous work demonstrated that Erk-mediated serine-phosphorylation activates and stabilizes p53 (Fuchs et al., 1998). Compared to wild-type pre-B ALL cells, $Dusp6^{-/-}$and $Etv5^{-/-}$ pre-B ALL cells expressed higher p53 protein levels (Figure 4B). 4-OHT-mediated induction of Cre in $Spry2^{fl/fl}$ pre-B ALL cells resulted in deletion of *Spry2* and rapid pre-B ALL cell death in parallel with hyperactive Erk signaling (Figures 4C–4E). The decrease in the number of cells in S phase likely reflects induction of cell death upon deletion of *Spry2* (Figure 4F). We confirmed that Erk-hyperactivation, resulting from loss of SPRY2 function, compromised pre-B ALL leukemogenesis in vivo. To this end, $Spry2^{fl/fl}$ pre-B ALL cells were transduced with either 4-OHT inducible Cre or an empty vector control (EV), labeled with firefly luciferase, and injected into sublethally irradiated nonobese diabetic (NOD)/severe combined immunodeficiency (SCID) recipient mice. $Spry2^{fl/fl}$ leukemia cells in Cre and EV groups were normalized for equal numbers (1 million) and luciferase signal intensity (Figure 4G) prior to injection. Consistent with in vitro findings, deletion of *Spry2* delayed leukemia onset in vivo and prolonged overall survival of NOD/SCID recipient mice. Since Erk activity increases levels of reactive oxygen species (ROS) via phosphorylation of $p47^{Phox}$-S^{359} (Dang et al., 2006), we examined the role of Erk negative control in ROS-regulation. Genetic deletion of *Dusp6*, *Etv5*, and *Spry2* in BCR-ABL1-transformed pre-B ALL cells caused significant accumulation of ROS (Figure 4H). In parallel with increased p53 protein levels in $Dusp6^{-/-}$ and $Etv5^{-/-}$ pre-B ALL cells, leukemia cells lacking robust Erk negative control lost colony forming ability in methylcellulose (Figure 4I).

DUSP6-Deficient Pre-B Cells Are Not Permissive to Transformation by BCR-ABL1

We next tested how calibration of Erk activity by DUSP6 and SPRY2 activity affects malignant transformation of pre-B cells. To test the role of DUSP6, we performed a TKI-washout experiment for acute activation of BCR-ABL1 in pre-B cells. $Dusp6^{+/+}$ and $Dusp6^{-/-}$ pre-B cells were propagated in the presence of IL7 and saturating concentrations of Imatinib. IL7-dependent $Dusp6^{+/+}$ and $Dusp6^{-/-}$ pre-B cells were transduced with $BCR\text{-}ABL1^{GFP}$-vectors in the continued presence of Imatinib. On the second day after transduction, IL7 was removed from cell cultures. As expected, subsequent washout of Imatinib (red arrow; Figure 4J) and inducible activation of BCR-ABL1 resulted in IL7-independence and leukemic transformation of $Dusp6^{+/+}$ $BCR\text{-}ABL1^{GFP}$ pre-B cells. In contrast to $Dusp6^{+/+}$ cells, $Dusp6^{-/-}$ pre-B cells failed to undergo BCR-ABL1-mediated transformation and did not outgrow nontransduced cells in the absence of IL7 (Figure 4J). In addition, $Dusp6^{-/-}$ pre-B ALL cells were more sensitive to acute BCR-ABL1 tyrosine kinase inhibition by Imatinib, compared to wild-type controls (Figure 4K). Likewise, Cre-mediated deletion of *Spry2* sensitized pre-B ALL cells to acute BCR-ABL1 tyrosine kinase inhibition (Figure 4L). Collectively, genetic experiments in $NRAS^{G12D}$- and BCR-ABL1-driven pre-B ALL demonstrate that robust negative feedback control of Erk signaling is critical to balance acute fluctuations of oncogenic signaling strength (e.g., washout and treatment with Imatinib). Previous work established that SPRY2, DUSP6, and ETV5 have important tumor suppressor functions in multiple types of cancer, which is in agreement with our findings in myeloid $Dusp6^{-/-}$ leukemia cells (Figure 2D). In contrast, however, pre-B ALL cells are

(G) Knockdown of DUSP6 in human ALL cells with short hairpin (sh)RNA. The knockdown efficiency and changes in ERK1/2 phosphorylation were measured by western blot.

(H) $KRAS^{G12V}$- and *MLL-AF4*-driven human ALL cells were transduced with shRNA vectors against DUSP6 or scrambled controls and plated in methylcellulose to study their colony formation ability. The scale bars represent 1 mm. The p values were calculated from t test.

(I) $Dusp6^{+/+}$ and $Dusp6^{-/-}$ pre-B cells were induced to express $NRAS^{G12D}$, labeled with firefly luciferase, and injected into sublethally irradiated NOD/SCID recipients (n = 7 per group). The leukemia burden was measured by luciferase bioimaging and overall survival of the mouse recipients was plotted by Kaplan-Meier analysis. The p value was calculated by log-rank test. All of the error bars represent SD.

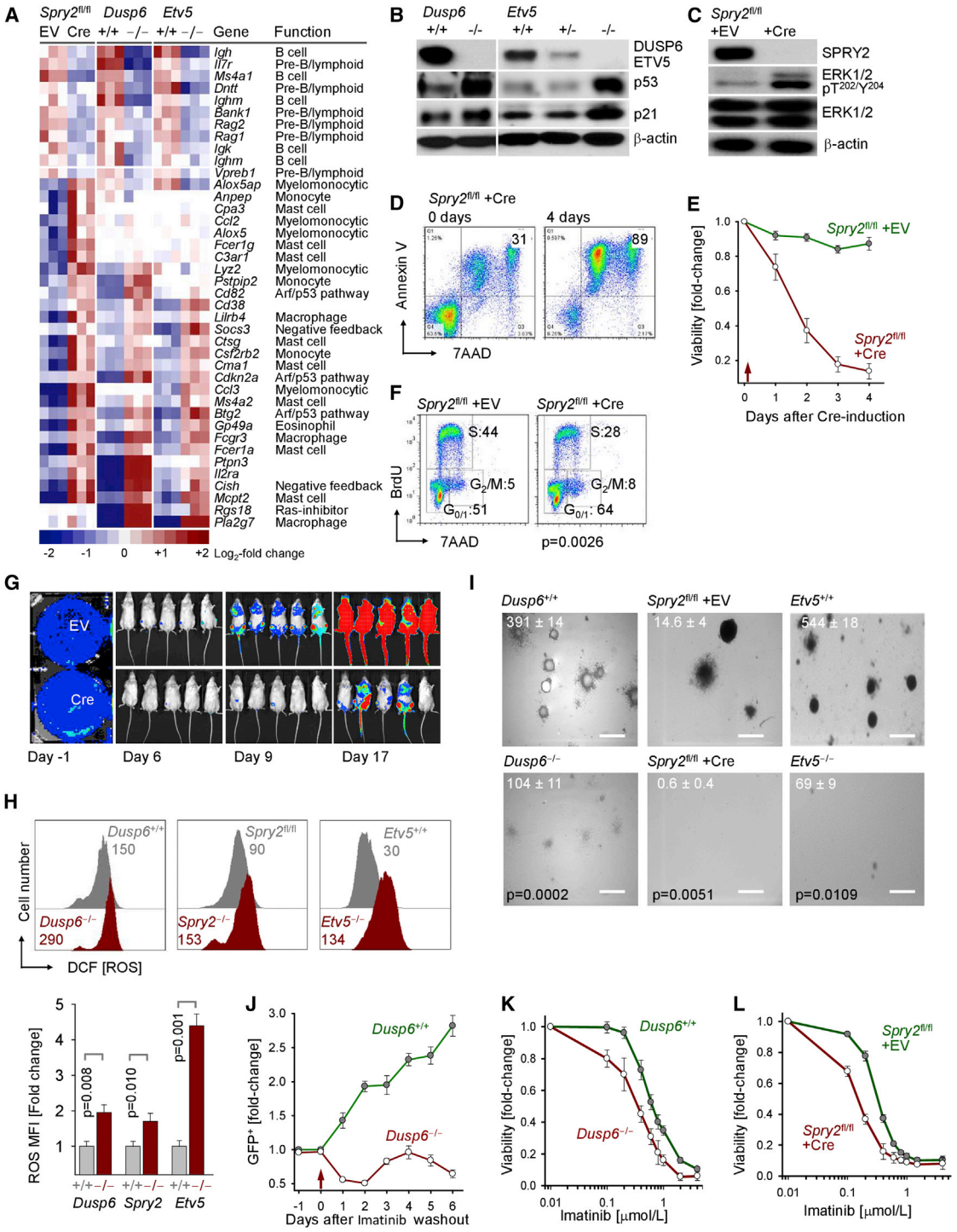

Figure 4. Genetic Analysis of Erk Negative Control in Pre-B ALL Cells

(A) Bone marrow pre-B cells from *Dusp6*$^{-/-}$, *Etv5*$^{-/-}$, and *Spry2*$^{fl/fl}$ mice and wild-type controls were transformed with BCR-ABL1. *Spry2*$^{fl/fl}$ leukemia cells were retrovirally transduced with a 4-OHT inducible Cre for deletion of LoxP-flanked *Spry2* alleles. The microarray analyses depict common gene expression changes upon loss of *Dusp6*, *Etv5*, and *Spry2* in pre-B ALL cells.

(B) Western blot analysis shows expression levels of p53 and p21 in BCR-ABL1 pre-B ALL cells lacking expression of *Dusp6* and *Etv5*.

(C) Inducible activation of Cre in *Spry2*$^{fl/fl}$ BCR-ABL1 pre-B ALL cells results in loss of SPRY2 expression and hyperactivation of Erk.

(D) Apoptosis was measured by flow cytometry (Annexin V^{+}).

(E) *Spry2*$^{fl/fl}$ ALL cells were retrovirally transduced with 4-OHT-inducible Cre and cell viability was monitored under cell culture conditions over time following 4-OHT addition.

(legend continued on next page)

uniquely dependent on the robust negative feedback control of Erk signaling.

Pharmacological Inhibition of DUSP6 in Human Pre-B ALL Cells

To explore potential targeting of negative regulatory signaling in human pre-B ALL, we tested a recently developed selective small molecule inhibitor of DUSP6, 2-benzylidene-3-(cyclohexylamino)-1-Indanone hydrochloride (BCI; Figure 5A; Vogt et al., 2003; Molina et al., 2009). As predicted, treatment of patient-derived Ph$^+$ ALL cells with BCI (5 μmol/l) resulted in hyperactivation of Erk within 1 hr (Figures 5B–5D). Interestingly, BCI-induced hyperactivation of Erk was paralleled by strong increases of ROS levels (Figure 5E). Small molecule inhibition of DUSP6 induced massive dephosphorylation at multiple phosphotyrosines as determined by global phospho-tyrosine analysis (Figure 5F). The net loss of tyrosine-phosphorylation events suggests that the initial peak of Erk hyperactivation is followed by loss of permissiveness to oncogenic tyrosine kinase signaling (BCR-ABL1; Figure 5F).

Our initial results indicated that pre-B cells are only permissive to strong oncogenic signaling (e.g., BCR-ABL1, NRAS^{G12D}) in the presence of robust negative control. In young BCR-ABL1-transgenic mice, pre-B cells carry a silent BCR-ABL1 oncogene until they have evolved robust negative regulation (Figures 1D–1F). Here, we observed that small molecule inhibition of DUSP6 compromises negative control of Erk signaling and obliterates oncogenic tyrosine kinase signaling (Figures 5F and 5G). Treatment with BCI reduced both total BCR-ABL1 and phosphorylation of Y^{412} in the BCR-ABL1 activation loop (Figure 5G), which reflects loss of catalytic activity (Hantschel and Superti-Furga, 2004). Interestingly, inhibition of DUSP6 abruptly reduced phosphorylation of RPS6-S$^{235/236}$, which represents a downstream substrate of PI3K-Akt signaling (Figure 5G). RPS6 dephosphorylation clearly precedes reduction of BCR-ABL1 expression and activity and, therefore, likely represents an independent event. Since DUSP6 inhibition (BCI, 2 μmol/l) resulted in BCR-ABL1 tyrosine kinase inactivation, we tested whether BCI treatment cooperates with BCR-ABL1 TKI and found strong synergistic activity with Imatinib (Figure 5H). BCI induced cell death in BCR-ABL1 ALL cells (half maximal inhibitory concentration [IC$_{50}$] 2.1 μmol/l), and subtherapeutic doses of Imatinib (0.5 μmol/l) enhanced sensitivity of the leukemia cells to BCI (IC$_{50}$ 0.7 μmol/L; Figure 5H).

Pharmacological Inhibition of DUSP6 in Ph$^+$ ALL Cells Induces p53-Mediated Cell Death

Studying pre-B ALL cells from patient-derived bone marrow biopsies, we confirmed that BCI induced strong upregulation of both Arf and p53 to a comparable extent as in murine *Dusp6*$^{-/-}$ pre-B ALL cells (Figures 6A and 6B). In a genetic experiment based on inducible Cre-mediated deletion of *Cdkn2a* or *Trp53* in mouse BCR-ABL1 ALL cells, we demonstrated that BCI mediates its cytotoxic effect in part through p53 and Arf (Figure 6C). These findings raise the possibility that BCI-mediated Erk-hyperactivation causes serine-phosphorylation and stabilization of p53 (Fuchs et al., 1998), which then contributes to the selective toxic effect of BCI in pre-B ALL cells. Previous work demonstrated that Erk signaling could activate the DNA damage response via phosphorylation of ATM-S^{1981} and CHK2-T^{68} (Golding et al., 2007). Therefore, pre-B ALL cells from two patients (BLQ5 and LAX2) were treated with or without BCI and phosphorylation levels of ERK1/2-T^{202}/Y^{204}, ATM-S^{1981}, and CHK2-T^{68} were measured. Interestingly, BCI-induced Erk-hyperactivation mimics the function of a DNA damage sensor and induced activation of the DNA damage response including ATM and CHK2, upstream of p53 (Figure 6D).

BCI-induced cell death was in part rescued by the ROS scavenger catalase (Figure 6E) and further increased by the glutathione-S-transferase inhibitor BSO (Figure S4), indicating that ROS is in part responsible for induction of cell death in patient-derived Ph$^+$ ALL cells. The nicotinamide adenine dinucleotide phosphate (NADPH) oxidase complex, activated by its regulatory subunit p47^{phox}, represents an important source of ROS production and is activated by Erk-dependent phosphorylation of p47^{Phox}-S^{359} (Dang et al., 2006). Compared to normal bone marrow pre-B cells, p47^{phox} levels and activation are significantly lower in patient-derived Ph$^+$ ALL cells (Figure 6F), suggesting that Ph$^+$ ALL cells are less permissive to p47^{phox}-driven ROS production. The effect of BCI on ROS accumulation in part depends on p47^{phox} function, since p47^{phox}-deficient (*Ncf1*$^{-/-}$) mouse leukemia cells showed lower levels of ROS accumulation (Figure 6G) and are significantly less sensitive to BCI (Figure 6H).

(F) Proliferation and cell cycle phases were measured by BrdU incorporation. The p value was calculated by t test for the S phase.

(G) *Spry2*$^{fl/fl}$ pre-B ALL cells were labeled with firefly luciferase. There were two million *Spry2*$^{fl/fl}$ pre-B ALL cells carrying either 4-OHT inducible Cre or an EV that were treated with 4-OHT and subsequently injected into sublethally irradiated NOD/SCID recipient mice (n = 14). The equal luciferase signal intensities for Cre and EV-transduced *Spry2*$^{fl/fl}$ leukemia cells were verified prior to injection. The Cre-dependent deletion of *Spry2* prolonged survival of the recipient mice (p = 0.044). The p value was calculated by log-rank test.

(H) *Dusp6*-, *Etv5*-, and *Spry2*-deficient and wild-type BCR-ABL1 pre-B ALL cells were stained with 2′7′-dichlorofluorescein (DCF) diacetate which labels cells based on intracellular levels of ROS. The mean fluorescence intensities for DCF [ROS] are depicted. The p values were calculated by t test.

(I) Each 10,000 *Dusp6*-, *Etv5*-, and *Spry2*-deficient and wild-type BCR-ABL1 pre-B ALL cells were plated in methylcellulose for 10 days and morphology and numbers of colonies are shown. The scale bars represent 0.5 mm. The p values were calculated by t test.

(J) *Dusp6*$^{-/-}$ and *Dusp6*$^{+/+}$ bone marrow pre-B cells were isolated and propagated in the presence of IL7. After the expansion of *Dusp6*$^{-/-}$ and *Dusp6*$^{+/+}$ pre-B cells, Imatinib (1 μmol/l) was added and pre-B cells were transduced with BCR-ABL1^{GFP}. In the presence of Imatinib, percentages of BCR-ABL1^{GFP+} cells did not change. Upon washout of Imatinib and IL7 (arrow), the fraction of BCR-ABL1^{GFP+} cells were plotted for *Dusp6*$^{+/+}$ and *Dusp6*$^{-/-}$ pre-B cells as fold-change relative to baseline.

(K) Sensitivity to Imatinib was measured in *Dusp6*$^{-/-}$ and *Dusp6*$^{+/+}$ pre-B ALL cells.

(L) Sensitivity to Imatinib was measured in *Spry2*$^{fl/fl}$ BCR-ABL1 pre-B ALL cells with and without activation of Cre. All of the error bars represent SD. See also Figure S3.

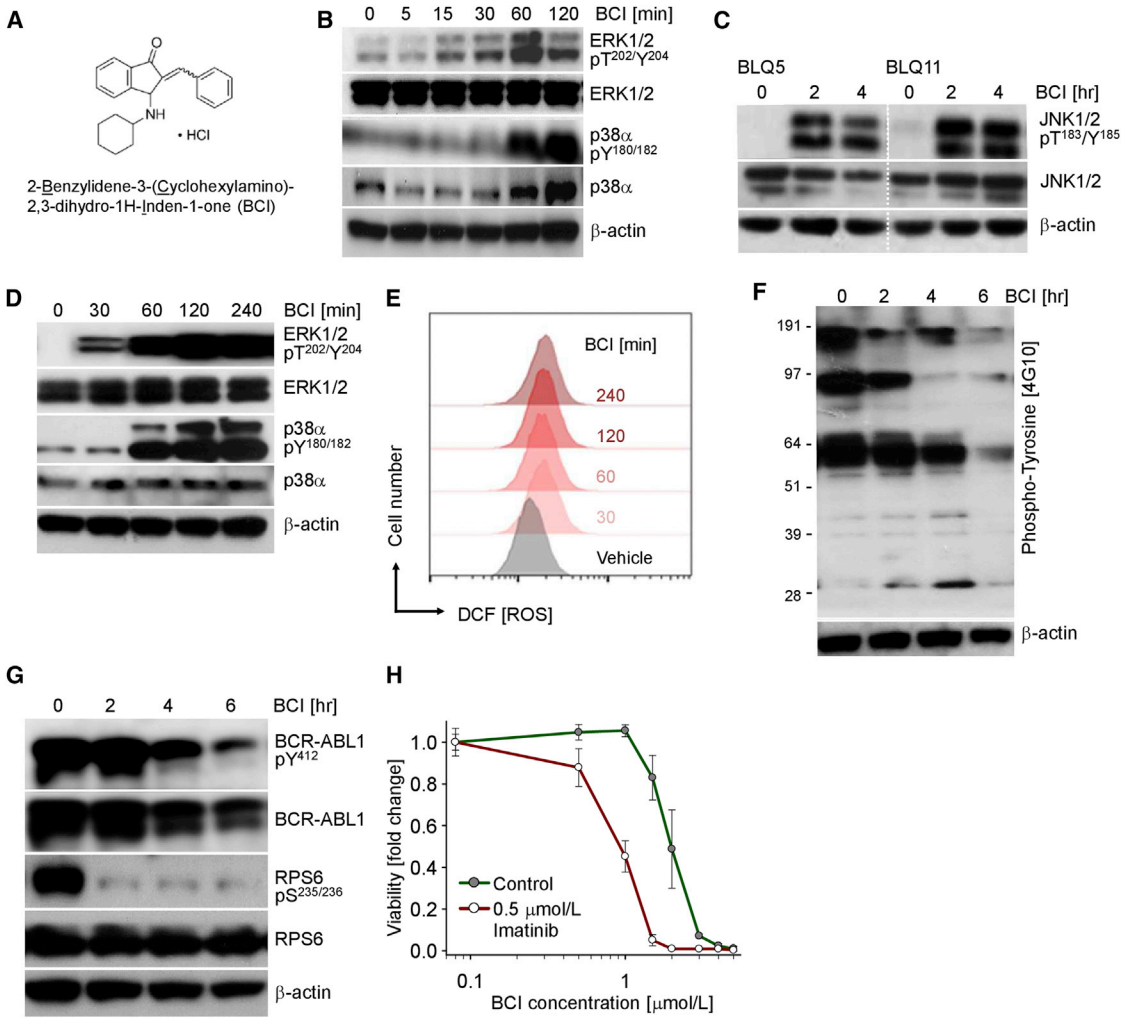

Figure 5. Pharmacological Inhibition of DUSP6-Mediated Erk Negative Control in Human Pre-B ALL Cells

(A) Chemical structure of selective DUSP6 inhibitor BCI.

(B) Time course analyses of BCI-treated patient-derived Ph^+ ALL cells (BLQ5) were performed for ERK1/2-pT^{202}/Y^{204}, total ERK1/2, p38α–pT^{180}/Y^{182}, and total p38α using β-actin as loading control.

(C) Time course analyses of BCI-treated patient-derived Ph^+ ALL cells were performed for JNK1pT^{183}/Y^{185} and total JNK1 using β-actin as loading control.

(D and E) Time course analyses of BCI-treated patient-derived Ph^+ pre-B ALL cells for ERK1/2 and p38α activity (D) and intracellular levels of ROS using 2′7′-dichlorofluorescein (DCF) diacetate (E).

(F) The effects of BCI on global phosphotyrosine.

(G) The effects of BCI on total and phosphorylated BCR-ABL1 and RPS6 as indicated.

(H) A dose-response analysis for BCI treatment and effects in viability of human Ph^+ ALL cells with or without combination with 0.5 μmol/l Imatinib was performed. The error bars represent SD.

DUSP6 Small Molecule Inhibition Can Overcome Drug-Resistance in Relapse Pre-B ALL

To test whether oncogenic activity of Erk confers selective sensitivity to DUSP6 inhibition, we studied patient-derived pre-B ALL cells that were isolated at the time of diagnosis (LAX7) and at the time of relapse (LAX7R), when pre-B ALL cells had acquired a *KRAS*^{G12V} mutation (Figure 7A). As a likely consequence of the acquired *KRAS*^{G12V} mutation, we found oncogenic activation of Erk in LAX7R, but not LAX7 cells (Figure 7B). In the absence of detectable baseline activity of Erk, DUSP6 inhibition had no biochemical effects on LAX7 (*KRAS* wild-type). In contrast, constitutive Erk activity in the *KRAS*^{G12V} mutant LAX7R cells was strongly increased by treatment with BCI. Relapse pre-B ALL clones typically acquire a high level of drug-resistance during the initial course of treatment (Bhojwani and Pui, 2013). However, comparing *KRAS* wild-type LAX7 cells and *KRAS*^{G12V} mutant LAX7R cells, the relapse ALL cells had acquired sensitivity to BCI (Figure 7C). Given that ALL clones frequently acquire oncogenic lesions in the RAS pathway leading to hyperactivation of Erk (Irving et al., 2014), these findings suggest that small molecule inhibition of DUSP6 may be useful to overcome drug-resistance in these patients.

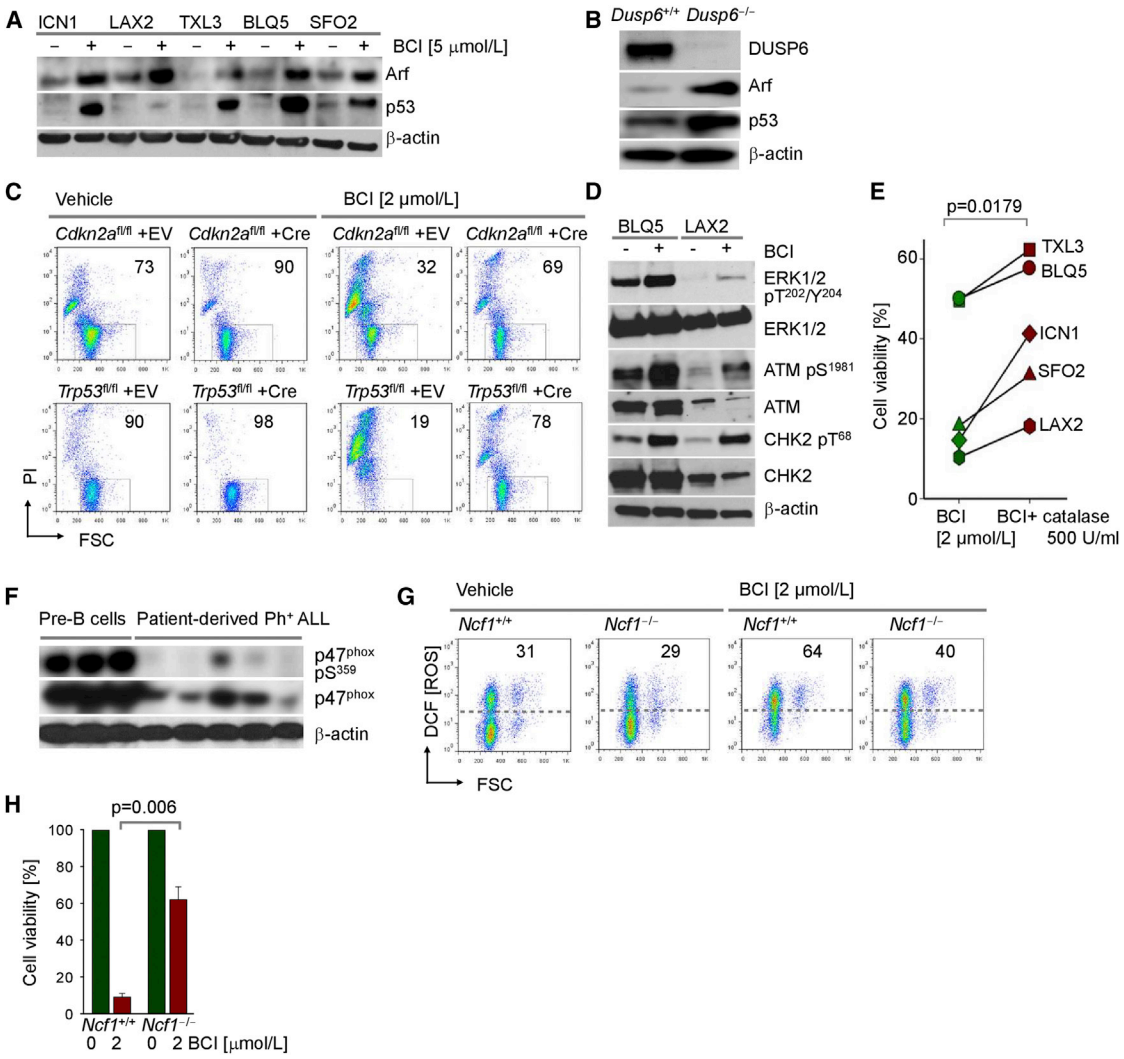

Figure 6. Pharmacological Inhibition of DUSP6 Induces Accumulation of ROS, Activation of DNA Damage Sensors, and Checkpoint Control Molecules in Ph+ ALL Cells

(A) Ph+ ALL cells from five patients were treated with 5 μmol/l BCI for 12 hr and were analyzed by western blot for expression of Arf and p53 expression using β-actin as loading control.

(B) Arf and p53 protein levels were compared by western blot in *Dusp6*$^{+/+}$ and *Dusp6*$^{-/-}$ pre-B ALL cells using β-actin as loading control.

(C) *Cdkn2a*$^{fl/fl}$ and *Trp53*$^{fl/fl}$ pre-B ALL cells carrying either 4-OHT inducible Cre or an EV were treated with 4-OHT, then with BCI for 2 days, and cell viability was measured by flow cytometry.

(D) Ph+ ALL cells from two patients were treated with 5 μmol/l BCI for 12 hr and total and phosphorylated proteins as indicated were measured by western blot.

(E) Ph+ ALL cells from five patients were treated with BCI or a combination of BCI and ROS-quencher catalase. The changes of viability comparing to the untreated cells were plotted on the y axis. The p value was calculated by t test.

(F) Normal bone marrow pre-B cells and primary Ph+ ALL cells were studied for expression and phosphorylation levels of p47^{phox} (S^{359}).

(G) *Ncf1*$^{+/+}$ and *Ncf1*$^{-/-}$ pre-B ALL cells were treated with BCI for 2 days and intracellular ROS levels were measured by flow cytometry.

(H) *Ncf1*$^{+/+}$ and *Ncf1*$^{-/-}$ pre-B ALL cells were treated with or without BCI for 2 days and viability changes relative to baseline (set as 100 percent; n = 3) were measured by flow cytometry. The error bars represent SD. The p value was calculated by t test. See also Figure S4.

Outcomes of DUSP6 Small Molecule Inhibition Depend on Apoptotic Thresholds of Erk Signaling

The selective effects of BCI on RAS mutant ALL cells with hyperactive Erk suggest that the BCI-induced toxicity is linked to a threshold of Erk signaling that has to be overcome to trigger apoptosis. To directly test this hypothesis, we experimentally lowered the "buffer setpoint" for Erk signaling and negative feedback control in patient-derived pre-B ALL cells expressing hyperactive Erk. To this end, LAX7R were cultured in the presence or absence of the MEK inhibitor PD0325901, the concentration of which was gradually increased from 0.1 nmol/l over 2 weeks to a final concentration of 50 nmol/l. At that time, PD0325901-treated cells had fully adapted to low levels of Erk signaling with similar viability and proliferation characteristics as vehicle-treated cells (Figure S5A). After washout of PD0325901 (Erk rebound), LAX7R cells were treated for 2 days

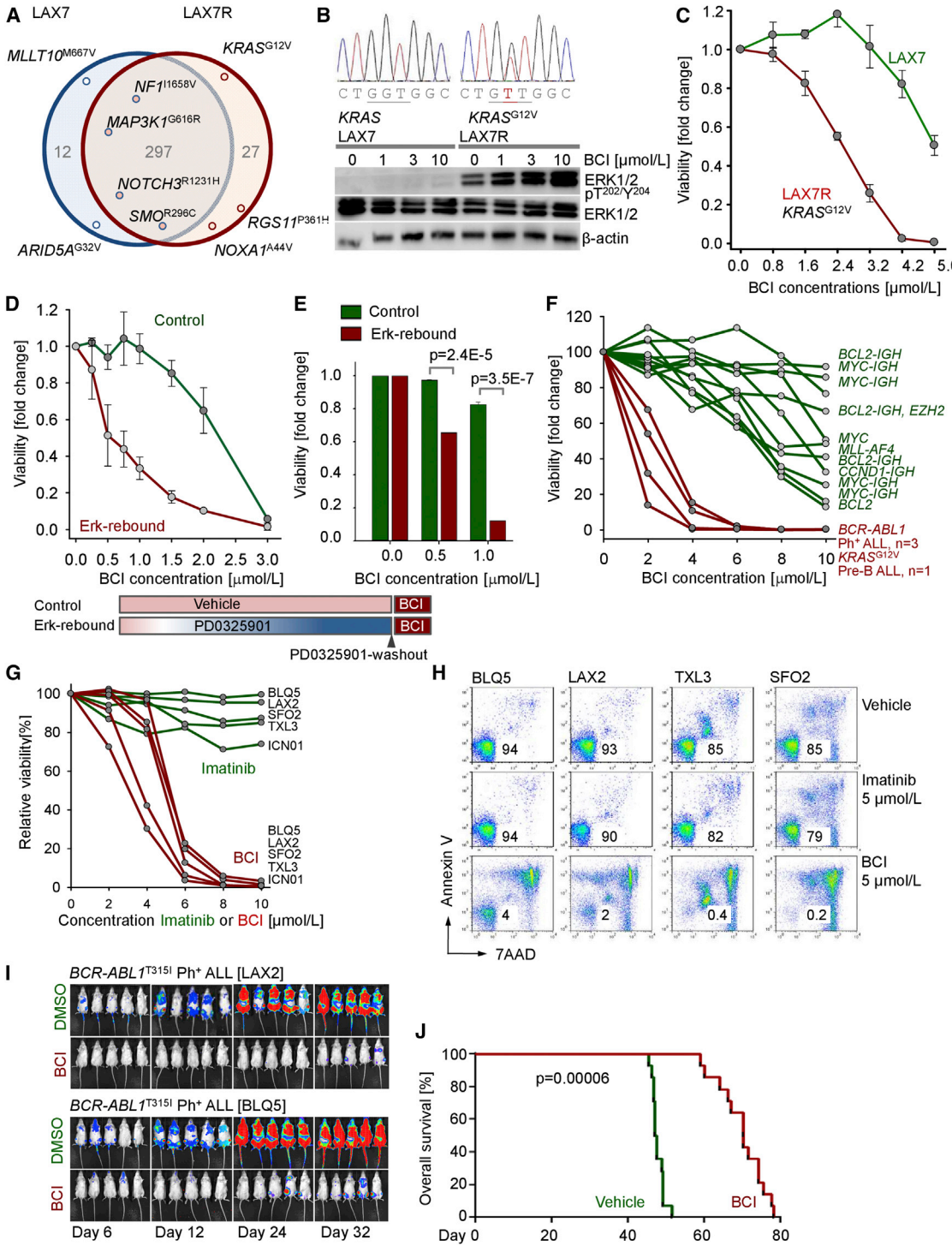

Figure 7. Small Molecule Inhibition of DUSP6 Overcomes TKI-Resistance in Ph+ ALL Cells

(A) Summary and representative mutations common between and unique to LAX7 and LAX7R identified by whole exome sequencing.

(B) Chromatogram showing the absence and the presence of the *KRAS*^{G12V} mutation in LAX7 and LAX7R cells, respectively, and western blot showing biochemical effects of BCI treatment on Erk activity.

(C) Viability of LAX7 and LAX7R cells incubated with BCI at various concentrations for 72 hr.

(D and E) Patient-derived Ph+ ALL cells growing in the presence of the control vehicle (control) or PD0325901 and washout of PD0325901 (Erk rebound) were treated for 2 days with BCI at various concentrations and their viability was measured by cell viability assay (D) or flow cytometry (E). The p values were calculated by t test.

(legend continued on next page)

with BCI at various concentrations and viability was measured. The "Erk-rebound" setting after initial lowering of Erk signaling thresholds (PD0325901-pretreatment) sensitized pre-B ALL cells to subsequent DUSP6 inhibition and reduced the IC_{50} for BCI from 2.3 μmol/l to 0.4 μmol/l (Figures 7D and 7E).

As expected, BCI selectively induced toxicity in a panel of human pre-B ALL cell lines expressing hyperactive Erk (Figure 7F). Given that Erk activity is usually low in normal cells, selective toxicity in cells expressing hyperactive Erk suggests a therapeutic window for pharmacological DUSP6 inhibition in pre-B ALL. For this reason, we tested the efficacy of BCI in a panel of five Ph^+ ALL xenografts from patients who relapsed during ongoing TKI-therapy (Figures 7G and 7H). While Imatinib-treatment did not significantly affect the viability of Ph^+ ALL cells from patients at the time of relapse, BCI achieved profound effects at the same dose levels (Figure 7G). Importantly, BCI was equally effective against Ph^+ ALL cells carrying the *BCR-ABL1*^{T315I} mutation, which confers Imatinib resistance (BLQ5 and LAX2; Figure 7G). To test whether DUSP6 inhibition can overcome Imatinib resistance of Ph^+ ALL cells in an in vivo setting, we labeled *BCR-ABL1*^{T315I} Ph^+ ALL cells from two patients (LAX2 and BLQ5) with firefly luciferase and injected them into sublethally irradiated (2.5 Gy) NOD/SCID mice. There were two different treatment schedules that were tested to examine the effect of BCI on leukemia-initiation (cells were treated for 4 hr before injection; Figures 7I and 7J) and on established leukemia (treatment started when leukemic expansion was visible by luciferase bioimaging; Figure S5B). For the latter, mice were treated with either vehicle, the second generation BCR-ABL1 TKI Nilotinib, or BCI. Mirroring drug-resistance in patients, treatment with Nilotinib did not significantly extend the lifespan of the transplanted mice (Figure S5B). By contrast, treatment with BCI significantly prolonged overall survival of the mice carrying established leukemia (Figure S5B). In summary, transplant studies of patient-derived Ph^+ ALL validated small molecule inhibition of DUSP6 and hyperactivation of Erk as a potentially useful approach for the treatment of TKI-resistant (e.g., *BCR-ABL1*^{T315I}) Ph^+ ALL.

DISCUSSION

In a wide range of solid tumors, acute hyperactivation of oncogenes including $BRAF^{V600E}$, Ras, and Myc can cause oncogene-induced senescence (Serrano et al., 1997; Michaloglou et al., 2005), which represents an important barrier against malignant transformation. Strong activation of negative feedback rather than hyperactive Erk signaling itself is responsible for induction of senescence and growth arrest in solid tumors (Courtois-Cox et al., 2006). In agreement with this concept, negative feedback regulation is typically disabled in advanced $BRAF^{V600E}$- and Ras-driven solid tumors (Pratilas et al., 2009) and gene encoding negative feedback regulators of Erk are frequently deleted, mutated, or hypermethylated in solid tumors and mature B cell lymphoma. Likewise, our findings in *Dusp6*$^{-/-}$ myeloid leukemia support the concept that negative regulators of Erk have an important role as tumor suppressors in attenuating oncogenic signaling (Courtois-Cox et al., 2006).

In contrast to the established tumor suppressor role of negative feedback in solid tumors, our study demonstrates that in pre-B ALL, robust negative feedback control of Erk is critical for oncogenic transformation and development of fatal disease. These findings suggest that negative control of Erk signaling represents a vulnerability and, potentially, a class of therapeutic targets in human pre-B ALL. Targeting negative regulation of Erk signaling for the treatment of pre-B ALL seems counterintuitive because it represents effectively the opposite of current efforts of targeted inhibition of oncogenic signaling. Besides the development of more potent TKI (Cortes et al., 2013), recent therapeutic concepts proposed the use of MEK inhibitors (Irving et al., 2014) to attenuate oncogenic Erk signaling in pre-B ALL. Our data using genetic mouse models and a small molecule inhibitor targeting DUSP6 demonstrate an unexpected addiction of pre-B ALL cells to Erk negative control. Normal cells lacking hyperactive Erk signaling are less dependent on negative feedback control of Erk and are spared, e.g., when treated with a small molecule inhibitor of DUSP6. If validated in pre-clinical studies, our approach of pharmacological blockade of Erk negative feedback control may result in the development of multiple targets for the therapy of pre-B ALL expressing hyperactive Erk (e.g., lesions in *NRAS*, *KRAS*, *BRAF*, *NF1*, and *PTPN11*; Zhang et al., 2011) and will broaden currently available treatment options.

A likely limitation of our proposed concept will be the development of drug-resistance. Current treatment regimens based on TKI or MEK inhibitors alone invariably select for drug-resistant subclones (Zabriskie et al., 2014). We expect that inhibitors of Erk negative control (e.g., DUSP6 inhibition by BCI) will likewise select for subclones that have acquired fitness to evade toxicity. However, we predict that the outcome of clonal selection will not confer adaptive fitness when selective pressures from opposite directions are applied sequentially. For instance, if a sequential treatment regimen begins with targeted inhibition of oncogene signaling (e.g., TKI or MEK inhibitor), leukemia cells may adapt to low oncogene signaling output by lowering the buffer setpoint for negative control. In this case, washout of TKI or MEK inhibitor and a subsequent round of pharmacological inhibition of negative control (e.g., using the DUSP6 inhibitor BCI) had more profound effects because selective pressures in the first round of treatment (TKI or MEK-inhibitor) did not confer adaptive fitness in the second treatment cycle (DUSP6 inhibitor BCI). While detailed studies are needed to optimize dosing and scheduling

(F) There were three Ph^+ ALL and one *KRAS*^{G12V} pre-B ALL cases (red lines) and 11 B cell lymphoma (green lines) that were treated with BCI at various concentrations for 72 hr and cell viability was measured by cell viability assay.

(G and H) Ph^+ ALL cells from five patients, including two cases with *BCR-ABL1*^{T315I} (BLQ5 and LAX2) were treated with TKI (Imatinib; green) or BCI (red curves) at various concentrations and viability was measured by cell viability assay (G) and flow cytometry (H).

(I and J) There were two patient-derived Ph^+ ALL cases carrying *BCR-ABL1*^{T315I} labeled with firefly luciferase that were treated with BCI (4 μmol/l) or vehicle for 4 hr then injected into sublethally irradiated NOD/SCID mice (one million cells each, n = 7 per group). The leukemia burden was measured by luciferase bioimaging (I). The overall survival of the recipient mice injected with LAX2 and BLQ5 is plotted as Kaplan-Meier analysis (J). The p value was calculated by log-rank test. All of the error bars represent SD. See also Figure S5.

of MEK inhibitors and BCI in an in vivo setting, these findings suggest that pharmacological blockade of Erk negative control represents a therapeutic concept that complements existing kinase inhibitor-based approaches. Moreover, the sequential use of pharmacological inhibition and hyperactivation of Erk may be useful to obviate clonal evolution that would otherwise favor outgrowth of drug-resistant mutants.

EXPERIMENTAL PROCEDURES

Mouse Model for BCR-ABL1- and NRAS^{G12D} Pre-B ALL

Bone marrow cells from young age-matched mice were harvested and retrovirally transformed by BCR-ABL1 or NRAS^{G12D} in the presence of 10 ng IL7/ml (Peprotech). A summary of mouse strains used in this study and the detailed procedure for bone marrow extraction and retroviral transduction is described in Supplemental Information.

In Vivo Model for BCR-ABL1-Transformed ALL

BCR-ABL1-transformed ALL cells or human primary leukemia cells were labeled with a firefly luciferase and were injected via tail vein into sublethally irradiated NOD/SCID mice. Bioimaging of leukemia progression in mice was performed at different time points using an in vivo IVIS 100 bioluminescence/optical imaging system (Xenogen). More details on in vivo injection and bioimaging are provided in the Supplemental Information. All mouse experiments were subject to institutional approval by the University of California San Francisco Institutional Animal Care and Use Committee. Patient derived leukemia samples were collected with informed consent from all participants according to National Cancer Institute/Cancer Therapy Evaluation Program (NCI/CTEP) approved protocol ECOG E2993T5 and studied with approval of the Institutional Review Boards of the University of California San Francisco (UCSF).

Proteomic Profiling

Proteomic profiling was performed using RPPA on peripheral blood and bone marrow specimens from 192 patients with ALL, including 192 samples at diagnosis and 12 paired diagnosis-relapse samples evaluated at The University of Texas M.D. Anderson Cancer Center (MDACC) between 1983 and 2007 (two from the 1980s and 45 from the 1990s). More details on the samples and the RPPA protocol are provided in the Supplemental Information.

Statistical Analysis

All pairwise comparisons between the means were calculated by two-tailed t test or Wilcoxon's rank-sum test using R software (R Development Core Team 2009; http://www.r-project.org). Comparison of patient survival data was carried out using log-rank test. A confidence coefficient of 0.05 was used for the all tests.

ACCESSION NUMBERS

The gene expression microarray data reported in this paper have been deposited in the NCBI Gene Expression Omnibus (GEO) (http://www.ncbi.nlm.nih.gov/geo) database with the GEO accession numbers GSE34832, GSE34834, GSE34833, GSE23743, and GSE21664.

SUPPLEMENTAL INFORMATION

Supplemental Information includes Supplemental Experimental Procedures and five figures and can be found with this article online at http://dx.doi.org/10.1016/j.ccell.2015.05.008.

AUTHOR CONTRIBUTIONS

S. Shojaee and M.M. designed experiments and interpreted data. M.M. conceived the study and wrote the paper. S. Shojaee, R.C., M.B., E. Park, C.H., H.G., L.K., and S. Swaminathan performed experiments and analyzed data. W.-K.H., A.M., E. Paietta, S.P.H., H.P.K., C.L.W., Y.H.Q., N.Z., K.R.C., and S.M.K. provided and characterized patient samples or cell lines and clinical outcome data. J.M. provided important reagents and mouse samples. J.M., H.P.K., S.P.H., C.L.W., and S.M.K. provided conceptual input to the design of the study as well as expertise in TKI treatment for leukemia and solid tumors.

ACKNOWLEDGMENTS

We thank Dr. Kenneth M. Murphy, St. Louis, MO and Dr. Gail R. Martin, San Francisco, CA for sharing *Etv5*$^{-/-}$ and *Spry2*$^{fl/fl}$ mice with us. This work is supported by grants from the NIH/NCI through R01CA137060, R01CA139032, R01CA169458, R01CA172558, and R01CA157644 (to M.M.); grants from the Leukemia and Lymphoma Society (to M.M.); the California Institute for Regenerative Medicine through TR02-1816 (M.M.); and the William Lawrence and Blanche Hughes Foundation and a Leukemia and Lymphoma Society SCOR grant (LLS-7005-11). M.M. is a Scholar of The Leukemia and Lymphoma Society and a Senior Investigator of the Wellcome Trust.

Received: July 3, 2014
Revised: February 5, 2015
Accepted: May 12, 2015
Published: June 11, 2015

REFERENCES

Bhojwani, D., and Pui, C.H. (2013). Relapsed childhood acute lymphoblastic leukaemia. Lancet Oncol. *14*, e205–e217.

Chen, C., Ouyang, W., Grigura, V., Zhou, Q., Carnes, K., Lim, H., Zhao, G.Q., Arber, S., Kurpios, N., Murphy, T.L., et al. (2005). ERM is required for transcriptional control of the spermatogonial stem cell niche. Nature *436*, 1030–1034.

Chi, P., Chen, Y., Zhang, L., Guo, X., Wongvipat, J., Shamu, T., Fletcher, J.A., Dewell, S., Maki, R.G., Zheng, D., et al. (2010). ETV1 is a lineage survival factor that cooperates with KIT in gastrointestinal stromal tumours. Nature *467*, 849–853.

Cortes, J.E., Kim, D.W., Pinilla-Ibarz, J., le Coutre, P., Paquette, R., Chuah, C., Nicolini, F.E., Apperley, J.F., Khoury, H.J., Talpaz, M., et al.; PACE Investigators (2013). A phase 2 trial of ponatinib in Philadelphia chromosome-positive leukemias. N. Engl. J. Med. *369*, 1783–1796.

Courtois-Cox, S., Genther Williams, S.M., Reczek, E.E., Johnson, B.W., McGillicuddy, L.T., Johannessen, C.M., Hollstein, P.E., MacCollin, M., and Cichowski, K. (2006). A negative feedback signaling network underlies oncogene-induced senescence. Cancer Cell *10*, 459–472.

Dang, P.M.-C., Stensballe, A., Boussetta, T., Raad, H., Dewas, C., Kroviarski, Y., Hayem, G., Jensen, O.N., Gougerot-Pocidalo, M.-A., and El-Benna, J. (2006). A specific p47phox -serine phosphorylated by convergent MAPKs mediates neutrophil NADPH oxidase priming at inflammatory sites. J. Clin. Invest. *116*, 2033–2043.

Druker, B.J., Sawyers, C.L., Kantarjian, H., Resta, D.J., Reese, S.F., Ford, J.M., Capdeville, R., and Talpaz, M. (2001). Activity of a specific inhibitor of the BCR-ABL tyrosine kinase in the blast crisis of chronic myeloid leukemia and acute lymphoblastic leukemia with the Philadelphia chromosome. N. Engl. J. Med. *344*, 1038–1042.

Fielding, A.K. (2010). How I treat Philadelphia chromosome-positive acute lymphoblastic leukemia. Blood *116*, 3409–3417.

Frank, M.J., Dawson, D.W., Bensinger, S.J., Hong, J.S., Knosp, W.M., Xu, L., Balatoni, C.E., Allen, E.L., Shen, R.R., Bar-Sagi, D., et al. (2009). Expression of sprouty2 inhibits B-cell proliferation and is epigenetically silenced in mouse and human B-cell lymphomas. Blood *113*, 2478–2487.

Fuchs, S.Y., Adler, V., Pincus, M.R., and Ronai, Z. (1998). MEKK1/JNK signaling stabilizes and activates p53. Proc. Natl. Acad. Sci. USA *95*, 10541–10546.

Golding, S.E., Rosenberg, E., Neill, S., Dent, P., Povirk, L.F., and Valerie, K. (2007). Extracellular signal-related kinase positively regulates ataxia telangiectasia mutated, homologous recombination repair, and the DNA damage response. Cancer Res. *67*, 1046–1053.

Hanafusa, H., Torii, S., Yasunaga, T., and Nishida, E. (2002). Sprouty1 and Sprouty2 provide a control mechanism for the Ras/MAPK signalling pathway. Nat. Cell Biol. *4*, 850–858.

Hantschel, O., and Superti-Furga, G. (2004). Regulation of the c-Abl and Bcr-Abl tyrosine kinases. Nat. Rev. Mol. Cell Biol. *5*, 33–44.

Hollenhorst, P.C., Ferris, M.W., Hull, M.A., Chae, H., Kim, S., and Graves, B.J. (2011). Oncogenic ETS proteins mimic activated RAS/MAPK signaling in prostate cells. Genes Dev. *25*, 2147–2157.

Irving, J., Matheson, E., Minto, L., Blair, H., Case, M., Halsey, C., Swidenbank, I., Ponthan, F., Kirschner-Schwabe, R., Groeneveld-Krentz, S., et al. (2014). Ras pathway mutations are prevalent in relapsed childhood acute lymphoblastic leukemia and confer sensitivity to MEK inhibition. Blood *124*, 3420–3430.

Limnander, A., Depeille, P., Freedman, T.S., Liou, J., Leitges, M., Kurosaki, T., Roose, J.P., and Weiss, A. (2011). STIM1, PKC-δ and RasGRP set a threshold for proapoptotic Erk signaling during B cell development. Nat. Immunol. *12*, 425–433.

Maillet, M., Purcell, N.H., Sargent, M.A., York, A.J., Bueno, O.F., and Molkentin, J.D. (2008). DUSP6 (MKP3) null mice show enhanced ERK1/2 phosphorylation at baseline and increased myocyte proliferation in the heart affecting disease susceptibility. J. Biol. Chem. *283*, 31246–31255.

Michaloglou, C., Vredeveld, L.C., Soengas, M.S., Denoyelle, C., Kuilman, T., van der Horst, C.M., Majoor, D.M., Shay, J.W., Mooi, W.J., and Peeper, D.S. (2005). $BRAF^{E600}$-associated senescence-like cell cycle arrest of human naevi. Nature *436*, 720–724.

Molina, G., Vogt, A., Bakan, A., Dai, W., Queiroz de Oliveira, P., Znosko, W., Smithgall, T.E., Bahar, I., Lazo, J.S., Day, B.W., and Tsang, M. (2009). Zebrafish chemical screening reveals an inhibitor of Dusp6 that expands cardiac cell lineages. Nat. Chem. Biol. *5*, 680–687.

Murphy, S.L., Xu, J., and Kochanek, K.D. (2013). Deaths: Final data for 2010. National vital statistics reports from the U.S. Department of Health and Human Services, Natl. Vital Stat. Rep. *61*, 1–117.

Pratilas, C.A., Taylor, B.S., Ye, Q., Viale, A., Sander, C., Solit, D.B., and Rosen, N. (2009). (V600E)BRAF is associated with disabled feedback inhibition of RAF-MEK signaling and elevated transcriptional output of the pathway. Proc. Natl. Acad. Sci. USA *106*, 4519–4524.

Roberts, K.G., Morin, R.D., Zhang, J., Hirst, M., Zhao, Y., Su, X., Chen, S.-C., Payne-Turner, D., Churchman, M.L., Harvey, R.C., et al. (2012). Genetic alterations activating kinase and cytokine receptor signaling in high-risk acute lymphoblastic leukemia. Cancer Cell *22*, 153–166.

Roberts, K.G., Li, Y., Payne-Turner, D., Harvey, R.C., Yang, Y., Pei, D., McCastlain, K., Ding, L., Lu, C., Song, G., et al. (2014). Targetable kinase-activating lesions in Ph-like acute lymphoblastic leukemia. N. Engl. J. Med. *371*, 1005–1015.

Schutzman, J.L., and Martin, G.R. (2012). Sprouty genes function in suppression of prostate tumorigenesis. Proc. Natl. Acad. Sci. USA *109*, 20023–20028.

Serrano, M., Lin, A.W., McCurrach, M.E., Beach, D., and Lowe, S.W. (1997). Oncogenic ras provokes premature cell senescence associated with accumulation of p53 and p16INK4a. Cell *88*, 593–602.

Shaw, A.T., Meissner, A., Dowdle, J.A., Crowley, D., Magendantz, M., Ouyang, C., Parisi, T., Rajagopal, J., Blank, L.J., Bronson, R.T., et al. (2007). Sprouty-2 regulates oncogenic K-ras in lung development and tumorigenesis. Genes Dev. *21*, 694–707.

Shim, K., Minowada, G., Coling, D.E., and Martin, G.R. (2005). Sprouty2, a mouse deafness gene, regulates cell fate decisions in the auditory sensory epithelium by antagonizing FGF signaling. Dev. Cell *8*, 553–564.

Tanoue, T., Adachi, M., Moriguchi, T., and Nishida, E. (2000). A conserved docking motif in MAP kinases common to substrates, activators and regulators. Nat. Cell Biol. *2*, 110–116.

Vogt, A., Cooley, K.A., Brisson, M., Tarpley, M.G., Wipf, P., and Lazo, J.S. (2003). Cell-active dual specificity phosphatase inhibitors identified by high-content screening. Chem. Biol. *10*, 733–742.

Voncken, J.W., Morris, C., Pattengale, P., Dennert, G., Kikly, C., Groffen, J., and Heisterkamp, N. (1992). Clonal development and karyotype evolution during leukemogenesis of BCR/ABL transgenic mice. Blood *79*, 1029–1036.

Wong, V.C.L., Chen, H., Ko, J.M.Y., Chan, K.W., Chan, Y.P., Law, S., Chua, D., Kwong, D.L.-W., Lung, H.L., Srivastava, G., et al. (2012). Tumor suppressor dual-specificity phosphatase 6 (DUSP6) impairs cell invasion and epithelial-mesenchymal transition (EMT)-associated phenotype. Int. J. Cancer *130*, 83–95.

Xu, S., Furukawa, T., Kanai, N., Sunamura, M., and Horii, A. (2005). Abrogation of DUSP6 by hypermethylation in human pancreatic cancer. J. Hum. Genet. *50*, 159–167.

Zabriskie, M.S., Eide, C.A., Tantravahi, S.K., Vellore, N.A., Estrada, J., Nicolini, F.E., Khoury, H.J., Larson, R.A., Konopleva, M., Cortes, J.E., et al. (2014). BCR-ABL1 compound mutations combining key kinase domain positions confer clinical resistance to ponatinib in Ph chromosome-positive leukemia. Cancer Cell *26*, 428–442.

Zhang, J., Mullighan, C.G., Harvey, R.C., Wu, G., Chen, X., Edmonson, M., Buetow, K.H., Carroll, W.L., Chen, I.-M., Devidas, M., et al. (2011). Key pathways are frequently mutated in high-risk childhood acute lymphoblastic leukemia: a report from the Children's Oncology Group. Blood *118*, 3080–3087.

Znosko, W.A., Yu, S., Thomas, K., Molina, G.A., Li, C., Tsang, W., Dawid, I.B., Moon, A.M., and Tsang, M. (2010). Overlapping functions of Pea3 ETS transcription factors in FGF signaling during zebrafish development. Dev. Biol. *342*, 11–25.